Channel Estimation and Equalization Algorithm for OFDM-Based Underwater Acoustic Communications Systems

Mhd Tahssin Altabbaa

Department of Electrical and Electronics Engineering
Kadir Has University
34083, Istanbul, Turkey
Email: tahsin.altabbaa@khas.edu.tr

Erdal Panayirci

Department of Electrical and Electronics Engineering
Kadir Has University
34083, Istanbul, Turkey
Email: eepanay@khas.edu.tr

***Abstract*—This paper is concerned with a challenging problem of channel estimation and equalization for orthogonal frequency division multiplexing (OFDM) systems in underwater acoustic (UWA) communications in the presence of Rician fading. The ambient noise is modeled as a correlated Gaussain noise. We combine the matching pursuit (MP), for the Doppler shift and the channel path delays estimation, along with the maximum a posteriori (MAP) estimation for the channel path gains and call the resulting algorithm MP-MAP algorithm. As a prior distribution for the sparse complex-valued channel gains, we choose a Rician distribution with unknown means and variances. They are in turn estimated by the maximum likelihood technique. After the channel equalization, detection of data is implemented at the receiver. Computer simulations show that the UWA channel is estimated very effectively and the proposed algorithm exhibits excellent symbol error rate and channel estimation performance.**

Keywords–Underwater acoustic communications; channel estimation; equalization; detection.

I. INTRODUCTION

Due to the importance of underwater acoustic (UWA) wireless communications, numerous proposals that deal with the impairments experienced in such environment have received quite an attention, especially in the last ten years. Several underwater applications such as natural disasters predictors, coastal radars, incoming near-field tsunami waves, and volcanic activity require underwater wireless communication, where acoustic signals are recognized as the best candidate for such implementations [1] [2]. However, UWA communication systems face several challenges such as low speed, long propagation delay, multipath and fading, and time dependent Doppler effects. Deployment of orthogonal frequency division multiplexing (OFDM)-based communication systems for underwater wireless communication is considered to be promising due to its robustness against large multipath spreads [3] [4].

Different related studies on UWA communications have been proposed. Many related studies over different UWA disciplines such as channel and Doppler estimation and noise mitigation algorithms are investigated upon realistic and synthetic data. In [5], the authors model the delay spread of an UWA channel. The proposed study shows a better channel impulse response (CIR) modeling when out-of-plane scattering and reverberation are taken into account. The authors of [6] proposed an algorithm where the receiver can detect the impulsive noise positions using the signal amplitude in the time domain, and the impulsive noise and the Doppler shift estimation are based on the null subcarriers of the OFDM symbol. A channel estimation for relay-based UWA systems is investigated in [7]. The authors considered a sparse CIR and a non-Gaussian channel gains in their channel model. The expectation-maximization (EM) along with the matching pursuit (MP) algorithms were employed for the Doppler shift and the delay estimation. In [8], the authors adopted superposition coding with OFDM for downlink communication in the presence of multiple stations (sensors). Based on statistical representation of each underwater station's channel state information (CSI), a resource allocation mechanism is proposed that obtains the transmitting power of each subcarrier for each user. An adaptive channel estimator based on least squares (LS) and recursive least-squares (RLS) is proposed in [9]. The results show a promising bit error rate (BER) performance and the average mean square error (MSE) can be obtained better than the linear minimum mean square error (LMMSE) or the LS. The authors of [10] investigated different modulation, channel estimation, and channel equalization techniques for OFDM-based and pilot-assisted UWA systems. They assumed in their simulations a channel that follows a Rayleigh distribution. Their results show that QPSK, DPSK, and 16QAM are the most suitable modulation schemes for UWA applications. The authors of [11] proposed a low computational complexity channel estimation algorithm based on fast block-Fourier transform (FFT) and orthogonal matching pursuit (OMP) in the presence of large pilot spacing. In [12], the authors proposed an OMP-based algorithm for channel coefficients estimation with no prior CSI knowledge in the presence of doubly selective channel.

In this paper, we assume a single-transmit and single-receive antennas and a parametric channel model that obeys a Rician distribution, where the CSI is known at the receiver. We model the ambient UWA noise as a correlated Gaussian noise whose correlation function fits well for realistic UWA channels. We then employ the MP algorithm on the oversampled version of the received signal for the estimation of the Doppler shift and the channel path delays of the UWA channel. Finally, we use the maximum *a posteriori* (MAP) technique to estimate the complex-valued sparse channel gains and the maximum likelihood (ML) technique to estimate the unknown

 ISBN: 978-1-61208-572-2

mean and variance parameters of the Rician distributed UWA channel.

The remainder of the paper is organized as follows. The underwater channel model is presented in Section II. In Section III, the system model of the proposed OFDM-based UWA communication system is described. The iterative channel estimation algorithm along with the initialization techniques and data detection are described in Section IV. The performance of the proposed approach along with the simulation parameters are investigated in Section V. Finally, conclusions and future work are presented in Section VI.

II. Channel Model

In this paper, we consider a sparse multipath channel model parametrized by a time-varying path delays denoted by $\tau_p, p = 0, 1, \cdots, L-1$. The time variations of the path delays can be approximated by a Doppler shift as $\tau_p(t) = \tau_p - \zeta_p t$ [13] [6]. Note that, the Doppler effect experienced at the receiver can be different at each path in underwater environments [14]. However, [15] states that the dominant Doppler shift arose in such environments is due to the motion of the platforms. Consequently, in our paper we assume a constant Doppler shift, that is, $\zeta_p(t) \equiv \zeta$. In addition, we assume the channel path amplitudes do not change over one OFDM symbol duration on each path and vary independently from symbol to symbol, that is, $h_p(t) \approx h_p$. Consequently, the sparse time-varying UWA channel impulse responses (CIRs) with the channel gains can be characterized by

$$h(t,\tau) = \sum_{p=0}^{L-1} h_p \ \delta(\tau - (\tau_p - \zeta t)). \tag{1}$$

The channel taps at the receiver depend on the underwater environmental conditions as well as the sea state where each channel tap can be assumed to obey a different distribution. In our work, the proposed channel path gains h_p follow a Rician fading, and the channel taps are then considered to be complex Gaussian random variables with nonzero means. Define mean μ_p and variance σ_p^2 as the independent real and imaginary parts of the taps such that, $\Omega_p = E\{|h_p|^2\} = 2\mu_p^2 + 2\sigma_p^2$ is the power profile of the proposed channel that follows a Rician fading, where $\sum_{p=0}^{L-1} \Omega_p = 1$. However, we consider the Rician κ-factor for the p^{th} tap as the ratio of the power of the mean component to the power in the diffuse component, that is, $\kappa_p = \mu_p^2/\sigma_p^2$. Consequently, each channel tap can be expressed as [16]

$$h_p = \sqrt{\frac{\kappa_p \Omega_p}{\kappa_p + 1}}\left(\frac{1+j}{\sqrt{2}}\right) + \sqrt{\frac{\Omega_p}{\kappa_p + 1}}\tilde{h}_p \tag{2}$$

where $\tilde{h}_p$ is denoted as a complex Gaussian random variable with zero mean and unit variance. However, a Rayleigh distributed channel model can be considered in (2) when $\kappa = 0$. In addition, we assume that the CIRs remain constant over a period of one block transmission and vary independently from block to block.

III. System Model

In this work, we consider a direct communication link in an UWA framework where OFDM scheme is chosen for its robustness against long multipath spread experienced in underwater environments, where the derivations and the equations hold only one OFDM symbol at a time. We assume the proposed OFDM symbol is equipped with N subcarriers; K equally spaced subcarriers are modulated by data symbol $d[k]$ along the system bandwidth B, where k represents the subcarrier index of the OFDM symbol, and no data is transmitted over the remaining $N - K$ subacarriers.

After applying a N-point inverse fast Fourier transform (IFFT) of the data sequence, a sufficient guard interval (cyclic prefix) of duration T_g is added. Consequently, the equivalent passband continuous time-domain received signal $y(t) = s(t) \otimes h(t,\tau) + v(t)$ can be expressed as

$$y(t) = \sqrt{2}\mathfrak{Re}\left\{\left(\sum_{p=0}^{L-1} h_p \ e^{j2\pi f_c \zeta t} S\right) e^{j2\pi f_c t}\right\} + v(t), \tag{3}$$

where $S = s\left((1+\zeta)\, t - \tau_p\right)$, and $v(t) = \sqrt{2}\,\mathfrak{Re}\{\tilde{v}(t) e^{j\omega_c t}\}$ is the passband representation of the additive correlative Gaussian ambient noise $\tilde{v}(t)$.

In order to compensate the dominant Doppler shift, we resample the received signal in (3) with a resampling factor of $(1 + \zeta)$. The resulting signal $y_{RS}(t)$ experiences a residual Doppler shift ϑ on each path around zero in the range of $[-\xi_{max}, \xi_{max}]$ [13]. Define $\xi \triangleq \vartheta f_c$ as the residual carrier frequency offset (CFO), and $\hat{\xi}$ as a finer estimator of ξ. Consequently, we perform another Doppler shift compensation via demodulation process resulting $z_{RS}(t) = y_{RS}(t) e^{-j2\pi\hat{\xi}t}$ [14].

Finally, after applying an A/D conversion, a guard interval removal, and a $N-$point FFT is performed to transform the signal to the frequency domain, the k^{th} subcarrier output of the FFT during any received OFDM symbol can be represented by

$$\begin{aligned} Z_{RS}[k] &= \frac{1}{\sqrt{N}} \sum_{n=0}^{N-1} z_{RS}[n] \ \exp(-j\frac{2\pi nk}{N}) \\ &= \sum_{q=-K/2}^{K/2-1} d_q H[k,q] + V_{RS}[k], \end{aligned} \tag{4}$$

where $k = -K/2, -K/2+1 \cdots, K/2-1$, and

$$H[k,q] = \sum_{p=0}^{L-1} h_p \exp(-j\frac{2\pi q \tilde{\tau}_p}{N}) F_{k,q}(\vartheta), \tag{5}$$

$$F_{k,q}(\vartheta) = \frac{\sin(\Theta_{k,q})}{N\sin(\Theta_{k,q}/N)} \exp\left(-j\frac{N-1}{N}\Theta_{k,q}\right), \tag{6}$$

where $\Theta_{k,q} = \pi\big(q(1+\vartheta) - k\big)$, and the frequency domain noise samples $V_{RS}[k] = (1/\sqrt{N}) \sum_{n=0}^{N-1} v_{RS}[n] \exp(-j\frac{2\pi nk}{N})$. Consequently, substituting (5) in (4), the vector form of (4) is given by

$$\mathbf{Z}_{RS} = \mathbf{H}\ \mathbf{d} + \mathbf{V}_{RS}, \tag{7}$$

where, $\mathbf{Z}_{RS}$, $\mathbf{d}$, and $\mathbf{V}_{RS} \in \mathcal{C}^K$ and the $[k,q]^{th}$ element of $\mathbf{H} \in \mathcal{C}^{K \times K}$ is determined from (5). It can be seen from (4) that the ambient noise vector $\mathbf{V}_{RS}$ is colored and a whitening process has to be carried out in order to proceed to the channel estimation procedure.

Define S as the power spectral density of the ambient noise modeled in the 10 - 100 KHz band as a function of frequency in Hz as

$$S(f) = \frac{f_0 \hat{\sigma}_0^2}{\pi(f^2 + f_0^2)} \ , \tag{8}$$

where $\hat{\sigma}_0^2$ is the noise variance, f_0 is chosen as a model parameter of the colored noise autocorrelation function ($f_0 T_s = 0.01, 0.05, 0.1, etc.$), and $R_v(t,t') = \hat{\sigma}_0^2 \, e^{-2\pi|t-t'|f_0 T_s}$ is defined as the autocorrelation function of the ambient noise.

It can be seen easily from (8) that the noise samples in $\mathbf{V}_{RS}$ are complex-valued and correlated Gaussian distributed random variables with zero-means. Hence, the autocorrelation function can be expressed as,

$$R_{v_{RS}}[m] = R_v\big(mT_s/(1+\hat{\zeta})\big) e^{-j\omega_c \frac{\hat{\zeta}}{1+\hat{\zeta}} m T_s}. \tag{9}$$

However, it can be seen that the noise of the resampled observation model in (4) is colored. Therefore, we perform a noise whitening process on the observation model (7) based on the singular value decomposition (SVD) of the noise covariance matrix as $\mathbf{R}_{\mathbf{V}_{RS}} = \mathbf{U}\boldsymbol{\Upsilon}\mathbf{U}^{\dagger}$, where $\boldsymbol{\Upsilon}$ is a $K \times K$ diagonal matrix with positive real entries, $\mathbf{U} \in \mathcal{C}^{K \times K}$ is a complex valued unitary transformation matrix, and $(\cdot)^{\dagger}$ denotes the conjugate transpose operator. Hence, the colored noise V_{RS} is transformed into a white Gaussian noise $\mathbf{W}$ vector whose components have zero mean and unit variance.

Define $\boldsymbol{\Psi} = \boldsymbol{\Upsilon}^{-1/2}\mathbf{U}^{\dagger} \in \mathcal{C}^{K \times K}$ as the whitening matrix, consequently, the observation model in (7) is multiplied by $\boldsymbol{\Psi}$ from the left, and the final form of the observation model can be expressed as

$$\mathbf{Z} = \mathbf{G}\mathbf{d} + \mathbf{W} \in \mathcal{C}^K \ , \tag{10}$$

where $\mathbf{Z} = \boldsymbol{\Psi}\,\mathbf{Z}_{RS} \in \mathcal{C}^K$, $\mathbf{W} \in \mathcal{C}^K$, and the convolution matrix generated from data symbols $\mathbf{G} = \boldsymbol{\Psi}\,\mathbf{H} \in \mathcal{C}^{K \times K}$.

IV. Sparse Multipath Channel Estimation

In this section, we present the proposed algorithm that aims to estimate the channel path delays, the Doppler spread, and the sparse complex-valued channel gains. From the observation vector $\mathbf{Z}$ in (10), and by means of the pilot data on subcarriers, $\{\mathcal{P} = \{p_1, p_2, \cdots, p_P\} \in \mathcal{K}\}$, the LS estimation technique yields,

$$\hat{G}[p_k, p_k] = \frac{Z[p_k]}{d_{p_k}} = G[p_k, p_k] + V[p_k], \tag{11}$$

where $V[p_k] = \sum_{q \in \mathcal{P}, q \neq p_k} d_q \, G[p_k, q] + W[p_k]$, and $G[p_k, q]$ represents the interference experienced among the subcarriers. Accordingly, using (5) and (6), (11) can be expressed as

$$\mathbf{Z}_P = \mathbf{A}_P \mathbf{h} + \mathbf{V}_P, \tag{12}$$

where $\mathbf{Z}_P = \big[\hat{G}[p_1, p_1], \hat{G}[p_2, p_2], \cdots, \hat{G}[p_P, p_P]\big]^T \in \mathcal{C}^P$, $\mathbf{V}_P = [v(p_1), v(p_2), \cdots, v(p_P)]^T \in \mathcal{C}^P$ and $\mathbf{A}_P \in \mathcal{C}^{P \times L}$ matrix is given by

$$\mathbf{A}_P = \begin{bmatrix} \eta_1(\vartheta) e^{-j2\pi p_1 \tilde{\tau}_0/N} & \cdots & \eta_1(\vartheta) e^{-j2\pi p_1 \tilde{\tau}_{L-1}/N} \\ \eta_2(\vartheta) e^{-j2\pi p_2 \tilde{\tau}_0/N} & \cdots & \eta_2(\vartheta) e^{-j2\pi p_2 \tilde{\tau}_{L-1}/N} \\ . & \cdots & . \\ . & \cdots & . \\ \eta_P(\vartheta) e^{-j2\pi p_P \tilde{\tau}_0/N} & \cdots & \eta_P(\vartheta) e^{-j2\pi p_P \tilde{\tau}_{L-1}/N} \end{bmatrix}, \tag{13}$$

where $\eta_r(\vartheta) = \sum_{k=-K/2}^{K/2-1} \psi_{r+K/2+1,\ k+K/2+1} \ F_{k,r}(\vartheta)$, and $\psi_{m,n}$ is the $(m,n)^{th}$ element of the matrix $\boldsymbol{\Psi}$.

A. Delays, Doppler Shift and Gain Estimation

We perform an oversampling operation on (13) with an oversampling rate $R_s^{(\varrho)} = \varrho/T_s$, where $\varrho = \{1, 2, \cdots\}$, and T_s is the sampling interval [7] [14].

Let $\mathcal{T}_p = \lfloor \varrho \ \tilde{\tau}_p \rfloor$ and $\varphi = \lfloor (\vartheta + \xi_{max})/\Delta\xi \rfloor$ defined as the discretized real-valued normalized path delays and the Doppler spread, respectively. Note that, $\mathcal{T}_p \in \{0, 1, 2, \cdots, N_\tau - 1\}$, $N_\tau = \varrho L_g$, $L_g = T_g/T_s$, $\varphi \in \{0, 1, 2, \cdots, N_\xi - 1\}$, and $N_\xi = (2\xi_{max})/\Delta\xi$. The columns of the oversampled matrix $\mathbf{A}_P^{(\varrho)} \in \mathcal{C}^{P \times N_\tau N_\xi}$ are denoted by $\tilde{\mathbf{a}}_c = \{\, \tilde{\mathbf{a}}_0, \tilde{\mathbf{a}}_1, \cdots, \tilde{\mathbf{a}}_{N_\tau N_\xi - 1} \,\}$ and correspond to different discrete multipath channel taps and Doppler shift positions. The MP algorithm is then applied using the observation at the pilots (11) [17]. Consequently, the received signal in (12) can be rewritten as

$$\mathbf{Z}_P = \mathbf{A}_{c_p} \mathbf{h} + \mathbf{V}_P, \tag{14}$$

where $\mathbf{A}_{c_p} = [\mathbf{a}_{c_0}, \mathbf{a}_{c_1}, \cdots, \mathbf{a}_{c_{L-1}}]$ is the vector holding the $\mathbf{a}_{c_p}$ column vector values taken from the finer resolution matrix $\mathbf{A}_c \in \mathcal{C}^{P \times L}$ that allocates the path delays and the Doppler shifts obtained from MP.

We employ the MAP technique for a better channel path gains $\{h_p\}_{p=0}^{L-1}$ estimation using the reduced dimensional observation model in (14) [7]. For *a priori* information of the channel path gains, we take a Rician distribution in which h_p's are complex Gaussian random variables, having independent real and imaginary parts with mean μ_p and variance σ_p^2 considering a constant Rician factor, $\kappa_p = \mu_p^2/\sigma_p^2$, for each multipath component. Consequently, the parametric form of the prior joint pdf of $\mathbf{h}$ is given by

$$f(\mathbf{h}|\tilde{\boldsymbol{\mu}}, \mathbf{s}) = \prod_{p=0}^{L-1} \frac{1}{\pi s_p} \exp\left(-\frac{1}{s_p} \mid h_p - \tilde{\mu}_p \mid^2 \right), \tag{15}$$

where $\tilde{\mu}_p = \mu_p \ (1 + j)$, $s_p = 2\sigma_p^2$ and $\tilde{\boldsymbol{\mu}} = [\tilde{\mu}_0, \tilde{\mu}_1, \cdots, \tilde{\mu}_{L-1}]^T$, $\mathbf{s} = [s_0, s_1, \cdots, s_{L-1}]^T$ are the parameters controlling the prior mean and variance of each channel coefficient h_p. For fixed values of the parameters governing the prior, the posterior density of the channel coefficients vector is complex Gaussian as follows:

$$p(\mathbf{h}|\mathbf{Z}_P, \tilde{\boldsymbol{\mu}}, \mathbf{s}) = \mathcal{CN}(\boldsymbol{\mu}_h, \boldsymbol{\Sigma}_h), \tag{16}$$

with $\boldsymbol{\mu}_h = \boldsymbol{\Sigma}_h\big(\beta \ \mathbf{A}_c^{\dagger} \ \mathbf{Z}_P + \boldsymbol{\Gamma}^{-1}\tilde{\boldsymbol{\mu}}\big)$, and $\boldsymbol{\Sigma}_h = \big(\beta \mathbf{A}_c^{\dagger}\mathbf{A}_c + \boldsymbol{\Gamma}^{-1}\big)^{-1}$, where $\boldsymbol{\Gamma} = \mathrm{diag}(\mathbf{s})$ and $\beta \equiv 1/\sigma_V^2$. Consequently, from (16), the MAP estimator for $\mathbf{h}$ can be expressed as

$$\begin{aligned} \hat{\mathbf{h}}_{MAP} &= \arg\max_{\mathbf{h}} f(\mathbf{h}|\tilde{\boldsymbol{\mu}}, \mathbf{s}) = \boldsymbol{\mu}_h \\ &= \big(\mathbf{A}_c^{\dagger} \ \mathbf{A}_c + \frac{1}{\beta}\boldsymbol{\Gamma}^{-1}\big)^{-1}\big(\mathbf{A}_c^{\dagger} \ \mathbf{Z}_P + \frac{1}{\beta}\boldsymbol{\Gamma}^{-1}\tilde{\boldsymbol{\mu}}\big). \end{aligned} \tag{17}$$

However, $\mathbf{A}_c^{\dagger}\mathbf{A}_c$ is a banded matrix; therefore, it can be approximated as

$$\mathbf{A}_c^{\dagger}\mathbf{A}_c = \mathrm{diag}\left(\parallel \mathbf{a}_{c_0} \parallel^2, \parallel \mathbf{a}_{c_1} \parallel^2 \cdots, \parallel \mathbf{a}_{c_{L-1}} \parallel^2\right). \tag{18}$$

Consequently, the matrix inversion in (17) can be expressed as,

$$\left(\mathbf{A}_c^{\dagger}\mathbf{A}_c + \frac{1}{\beta}\boldsymbol{\Gamma}^{-1}\right)^{-1} = \mathrm{diag}(\lambda_0, \lambda_1, \cdots, \lambda_{L-1}), \tag{19}$$

where $\lambda_p = (\beta \parallel \mathbf{a}_{c_p} \parallel^2 + 1/s_p)^{-1}$.

B. ML Estimation of the Parameters $\{\mu_p, \sigma_p^2\}$

In order to obtain the ML estimation of the variance $\boldsymbol{\sigma}^2$ and the mean $\boldsymbol{\mu}$ vectors of $\mathbf{h}$, we use the observation model obtained by MP in (14). Consequently, the mean coefficient can be expressed by

$$\left(\boldsymbol{\mu}_{ML}, \boldsymbol{\sigma}^2{}_{ML}\right) = \arg\max_{\mu,\sigma^2} \log p(\mathbf{Z}_P|\boldsymbol{\mu}, \boldsymbol{\sigma}^2). \quad (20)$$

where $p(\mathbf{Z}_P|\boldsymbol{\sigma}^2, \mu)$ can be evaluated by averaging it over $\mathbf{h}$ as follows,

$$p(\mathbf{Z}_P|\boldsymbol{\mu}, \boldsymbol{\sigma}^2) = \int_{\mathbf{h}} p(\mathbf{Z}_P|\mathbf{h}) p(\mathbf{h}|\boldsymbol{\mu}, \boldsymbol{\sigma}^2) d\mathbf{h}, \quad (21)$$

where $p(\mathbf{Z}_P|\mathbf{h}) \backsim \exp\left\{-\beta \parallel \mathbf{Z}_P - \mathbf{A}_c\mathbf{h} \parallel^2 \right\}$, and $p(\mathbf{h}|\boldsymbol{\mu}, \sigma^2)$ is given by (15). The integral of (21) with respect to $\mathbf{h}$ is computable and yields

$$p(\mathbf{Z}_P|\boldsymbol{\sigma}^2, \boldsymbol{\mu}) = \pi^{-P} \det\left(\mathbf{C}_z^{-1}\right) \exp\left\{ -(\mathbf{Z}_P - \mathbf{A}_{c0}\boldsymbol{\mu})^\dagger \mathbf{C}_z^{-1}(\mathbf{Z}_P - \mathbf{A}_{c0}\boldsymbol{\mu}) \right\}, \quad (22)$$

where, $\mathbf{A}_{c0} \equiv (1+j)\mathbf{A}_c$, $\mathbf{C}_z = \mathbf{A}_c\boldsymbol{\chi}\mathbf{A}_c^\dagger + (1/\beta)\mathbf{I}_P$ and $\boldsymbol{\chi} = \text{diag}\left(2\sigma_0^2, 2\sigma_1^2, \cdots, 2\sigma_{L-1}^2\right)$. Then, the log-likelihood of $\boldsymbol{\mu}$ and σ^2 is given by

$$\log p(\mathbf{Z}_P|\boldsymbol{\mu}, \boldsymbol{\sigma}^2) = (\mathbf{Z}_P - \mathbf{A}_{c0}\boldsymbol{\mu})^\dagger \mathbf{C}_z^{-1}(\mathbf{Z}_P - \mathbf{A}_{c0}\boldsymbol{\mu}) + \log\det(\mathbf{C}_z). \quad (23)$$

Hence, the ML estimate of $\boldsymbol{\mu}$ can be found by minimizing (23) and taking the gradient of $\log p(\mathbf{Z}_P|\boldsymbol{\mu}, \boldsymbol{\sigma}^2)$ with respect to $\boldsymbol{\mu}$ and setting the result to zero. Consequently, $\boldsymbol{\mu}$ can then be expressed as,

$$\hat{\boldsymbol{\mu}}_{\text{ML}} = \left(\mathbf{A}_{c_p 0}^\dagger \mathbf{C}_z^{-1} \mathbf{A}_{c0}\right)^{-1} \Re\{\mathbf{A}_{c_p 0}^\dagger \mathbf{C}_z^{-1} \mathbf{Z}_P\}, \quad (24)$$

where $\Re\{z\}$ denotes the real part of z. We can express $\mathbf{C}_z^{-1} = \left(\mathbf{A}_c\boldsymbol{\chi}\mathbf{A}_c^\dagger + (1/\beta)\mathbf{I}_P\right)^{-1}$ using the matrix inversion lemma as follows,

$$\mathbf{C}_z^{-1} = \beta\mathbf{I}_P - \beta\mathbf{A}_c(\mathbf{A}_c^\dagger\mathbf{A}_c + (1/\beta)\boldsymbol{\chi})^{-1}\ \mathbf{A}_c^\dagger. \quad (25)$$

Using the property in (18), then (25) can be expressed as,

$$\mathbf{C}_z^{-1} = \beta\mathbf{I}_P - \beta\ \mathbf{A}_c\ \boldsymbol{\Lambda}\ \mathbf{A}_c^\dagger, \quad (26)$$

where $\boldsymbol{\Lambda} = \text{diag}(\lambda_0, \cdots, \lambda_{L-1})$ with $\lambda_p = \left(\parallel \mathbf{a}_{c_p} \parallel^2 + 1/(2\beta\sigma_p^2)\right)^{-1}$. Substituting (26) in (24) and after some algebra, $\hat{\boldsymbol{\mu}}_{\text{ML}}$ takes the form

$$\hat{\boldsymbol{\mu}}_{\text{ML}} = \frac{1}{2}\text{diag}\big(\parallel \mathbf{a}_{c_0} \parallel^{-2}, \parallel \mathbf{a}_{c_1} \parallel^{-2} \cdots, \parallel \mathbf{a}_{c_{L-1}} \parallel^{-2}\big)\Re\{\mathbf{A}_{c_p}^\dagger \mathbf{Z}_P\}. \quad (27)$$

The ML estimate of $\boldsymbol{\sigma}^2$ can now be found. We substitute the $\hat{\boldsymbol{\mu}}$ obtained in (27) and by maximizing the objective function (23) with respect to $\boldsymbol{\sigma}^2$ as follows,

$$O(\hat{\boldsymbol{\mu}}_{\text{ML}}, \boldsymbol{\sigma}^2) = \arg\max_{\sigma^2} \log p\left(\mathbf{Z}_P|\hat{\boldsymbol{\mu}}_{\text{ML}}, \boldsymbol{\sigma}^2\right), \quad (28)$$

Employing the property obtained from (18) in (25) and by discarding the terms independent of $\boldsymbol{\sigma}^2$, (28) can be expressed as,

$$O(\hat{\boldsymbol{\mu}}_{\text{ML}}, \boldsymbol{\sigma}^2) = \sum_{p=0}^{L-1} \log\left(\parallel \mathbf{a}_{c_p} \parallel^2 \sigma_p^2 + \frac{1}{\beta}\right) - \beta\sum_{p=0}^{L-1}\left(|e_p|^2\lambda_p - \parallel \mathbf{b} \parallel^2\right), \quad (29)$$

where $\mathbf{b} \triangleq \mathbf{Z}_P - \mathbf{A}_{c0}\ \hat{\boldsymbol{\mu}}_{\text{ML}}$ and e_p is the p^{th} component of the vector $\mathbf{e} = \mathbf{A}_{c0}^\dagger\mathbf{b}$. We take the gradient of O with respect to σ_p^2, and we equate it to zero. Consequently, the ML estimate for $\boldsymbol{\sigma}^2$ can be expressed as,

$$\hat{\sigma}_{p,ML}^2 = \left(\frac{|e_p|^2\beta - \parallel \mathbf{a}_{c_p} \parallel^2}{2 \parallel \mathbf{a}_{c_p} \parallel^4 \beta}\right)^+, \quad (30)$$

where $[x]^+ \triangleq \max(0, x)$.

C. Equalization and Data Detection

In this subsection, we demonstrate the data detection technique at the receiver using the observation model presented in (10). The proposed OFDM model contains P known pilot symbols evenly inserted in the K subcarriers, that is, the data symbols $\mathbf{d} = [d_0, d_1, \cdots, d_{K-1}]^T$ denotes the known, $\mathbf{d}_P$, and the the unknown, $\mathbf{d}_D$, data symbols, where the pilot positions vector is denoted by $p_r, r = 1, 2, \cdots, P$. Consequently, (10) can be expressed as

$$\mathbf{Z}_P \ \triangleq\ \mathbf{Z} - \mathbf{G}\mathbf{d}_P \ =\ \mathbf{G}\mathbf{d}_D + \mathbf{V}_P. \quad (31)$$

Then, the equalized soft data symbols $\tilde{\mathbf{d}}_D$ are recovered at the output of a linear minimum mean square error (MMSE) equalizer as

$$\tilde{\mathbf{d}}_D = \mathbf{G}^\dagger\left(\mathbf{G}\mathbf{G}^\dagger + \gamma^{-1}\mathbf{I}_K\right)^{-1}\mathbf{Z}_P\ , \quad (32)$$

where γ is the signal-to-noise ratio (SNR), $\mathbf{Z}_P^{(r)}$ is calculated from (31) as $\mathbf{Z}_P^{(r)} = \mathbf{Z} - \mathbf{G}^{(r)}\mathbf{d}_P$, and the $[k, q]^{th}$ element of $\mathbf{G}$ is computed from (5) and (6) by replacing the aforementioned channel estimates $\{h_p, (\vartheta, \tilde{\tau}_p)\}_{p=0}^{L-1}$. However, a demodulation process is performed over the equalized data symbols using ML detection technique.

V. Simulation Results

We now present the performance of the proposed approach in this section. The UWA OFDM system specifications along with the UWA channel parameters are summarized in Table-I.

TABLE I. CHANNEL AND SIMULATION PARAMETERS

carrier frequency (f_c)	18 KHz
channel bandwidth (BW)	7 KHz
number of subcarriers (K)	512
OFDM symbol duration (T)	73.15 ms
Subcarrier spacing ($\Delta f := 1/T$)	13.67 Hz
guard interval duration (T_g)	35 ms
number of paths on the link ($L_\times$)	3
maximum Doppler shift (ϑ_{max})	$10^{-2}, 5\times10^{-3}, 10^{-3}$
Doppler spread resolution $\Delta\xi$	10^{-3}
modulation formats	QPSK, 16QAM
pilot spacing (Δ_p)	4
oversampling factor (ϱ)	8

We consider a comb-type pilot structure with equally spaced pilot subcarriers in each OFDM block in order to assess the channel estimator and equalize the channel rapid changes per block. The mean-square error (MSE) and symbol error rate (SER) performance are presented as a function of SNR in Figs. 1 and 2, respectively. The curves show a comparison in performance of the proposed model with the classical MP channel estimation technique in the presence of quadrature phase shift-keying (QPSK) and 16-ary quadrature amplitude modulation (16QAM) signaling formats.

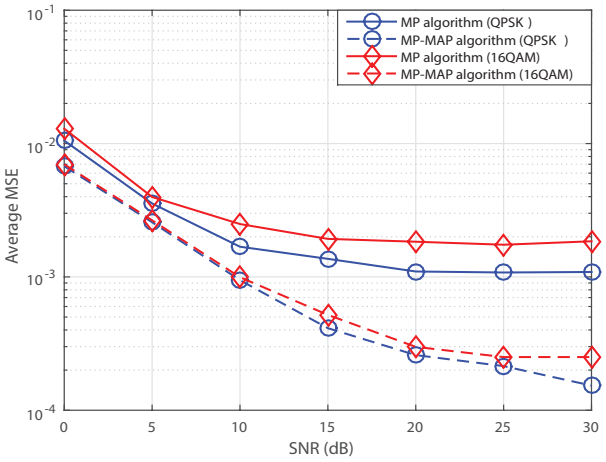

Figure 1. MSE vs. SNR performance comparisons of the MP-MAP and MP algorithms for different constellations: $\varrho = 8$, $\vartheta_{max} = 10^{-3}$

As seen from these two figures, the MP-MAP algorithm yields better channel MSE and SER performance and outperforms the MP estimator in the presence of higher SNR, where the MP curves shown use the linear MMSE equalizer to detect the data symbols.

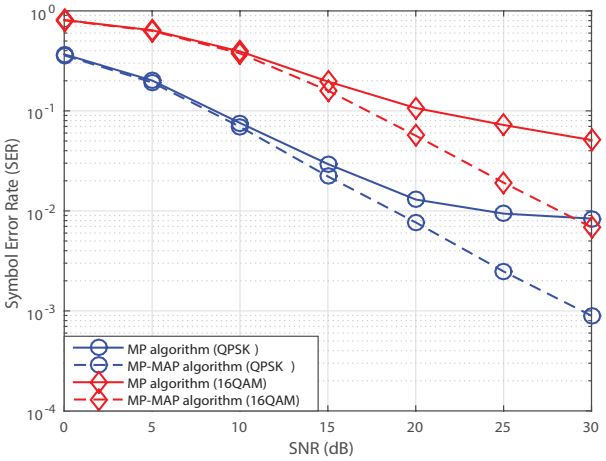

Figure 2. SER vs. SNR performance comparisons of the MP-MAP and MP algorithms for different constellations: $\varrho = 8$, $\vartheta_{max} = 10^{-3}$

Figs. 3 and 4 investigate the residual Doppler effect on the MSE and SER performance of the system as a function of SNR, respectively. It can be seen from these two figures that the performance of the channel estimator degrades with larger residual Doppler effect, whereas the curves of the proposed approach show better robustness compared to the MP algorithm alone against the Doppler shifts up to $\vartheta_{max} = 10^{-3}$, which can be considered as a severe Doppler effect.

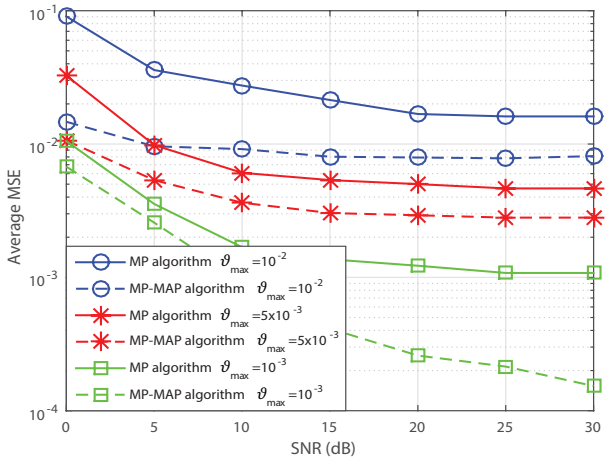

Figure 3. MSE vs. SNR performance of the MP-MAP algorithm for different Doppler shift rates, $\varrho = 8$, QPSK Signaling

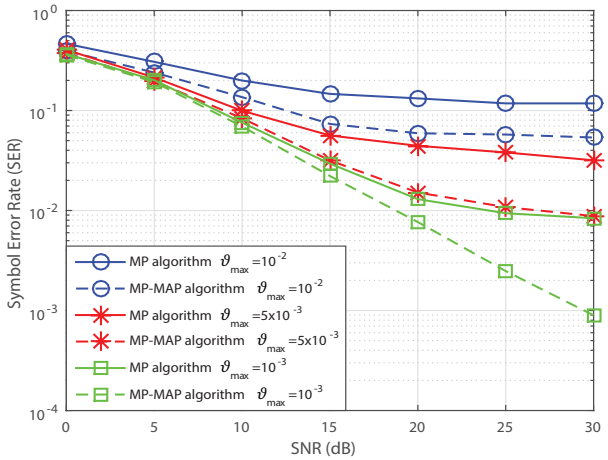

Figure 4. SER vs. SNR performance of the MP-MAP algorithm for different Doppler shift rates, $\varrho = 8$, QPSK Signaling

Note that, the value chosen for the oversampling factor assesses the underwater receiver with a firm Doppler shift and delay estimation and consequently a better MSE and SER performance.

VI. Conclusions and Future Work

In this work, an efficient channel estimation algorithm is proposed, named MP-MAP algorithm, for OFDM-based UWA systems in the presence of an UWA Rician channel with a correlated Gaussain noise. The channel delays and the Doppler shift are estimated by the matching pursuit algorithm, where the unknown parameters of the complex-valued channel gains are estimated by the maximum *a posteriori* algorithm. On the other hand, the variances and the means of the prior pdf of the channel gains are obtained by a ML estimation algorithm. The performance of the proposed approach is presented by means of the minimum mean square estimation of the estimated channel and the symbol error rate for different signaling formats and Doppler shifts. Based on the extensive computer simulations performed, it was concluded that the resulting MP-MAP channel estimation algorithm yields excellent MSE and SER performances as compared to the conventional approaches. For future work, the OFDM UWA communication system can be

 ISBN: 978-1-61208-572-2

generalized into MIMO-OFDM-based UWA communication system, and the proposed approach can be extended into an experimental channel model, taking into consideration a real underwater environment and parameters.

ACKNOWLEDGMENT

This research has been supported in part by Suasis as a sub-contract of the Turkish Scientific and Research Council (TUBITAK) under Grant 1140029.

REFERENCES

[1] N. Bahrami, N. H. H. Khamis, and A. B. Baharom, "Study of underwater channel estimation based on different node placement in shallow water," IEEE Sensors J., vol. 16, no. 4, pp. 1095-1102, Feb. 2016.

[2] B. Crosby, A. Rosenberger, and B. Pirenne, "The web-enabled awareness research network (WARN) project," in Proc. OCEANS 2015 - MTS/IEEE Washington, pp. 1-10, 2015

[3] E. V. Zorita and M. Stojanovic, "Space-frequency block coding for underwater acoustic communications," IEEE J. Ocean. Eng., vol. 40, no. 2, pp. 303-314, Apr. 2015.

[4] S. Akada, S. Yoshizawa, H. Tanimoto, and T. Saito, "Experimental evaluation of data selective rake reception for underwater acoustic communication," in Proc. 2015 International Symposium on Intelligent Signal Processing and Communication Systems, pp. 514-519, Nov. 2015.

[5] T. Jenserud and S. Ivansson, "Measurements and modeling of effects of out-of-plane reverberation on the power delay profile for underwater acoustic channels," IEEE J. Ocean. Eng., vol. 40, no. 4, pp. 807-821, Oct. 2015.

[6] X. Kuai, H. Sun, S. Zhou, and E. Cheng, "Impulsive noise mitigation in underwater acoustic OFDM systems," IEEE Trans. Veh. Technol., vol. 65, no. 10, pp. 8190-8202, Oct. 2016.

[7] E. Panayirci, H. Senol, M. Uysal, and V. Poor, "Sparse channel estimation and equalization for OFDM-based underwater cooperative systems with amplify-and-forward relaying," IEEE Trans. Signal Process., vol. 64, no. 1, pp. 214-228, Sept. 2016.

[8] L. Ma, S. Zhou, G. Qiao, S. Liu, and F. Zhou, "Superposition coding for downlink underwater acoustic OFDM," IEEE J. Ocean. Eng., vol. 42, no. 1, pp. 175-187, Jan. 2017.

[9] X. Shi and Y. Yang, "Adaptive sparse channel estimation based on RLS for underwater acoustic OFDM systems," in Proc. Sixth International Conference on Instrumentation and Measurement, Computer, Communication and Control, pp. 266-269, 2016.

[10] M. G. R. Kumar and M. Sarvagya, "Review on enhanced data rate receiver design using efficient modulation techniques for underwater acoustic communication," in Proc. 2016 International Conference on Advanced Communication Control and Computing Technologies, pp. 313-317, 2016.

[11] F. yu, D. Li, Q. Guo, Z. Wang, and W. Xiang, "Block-FFT based OMP for compressed channel estimation in underwater acoustic communications," IEEE Commun. Lett., vol. 19, no. 11, pp. 1937-1940, Nov. 2015.

[12] B. Peng, P. S. Rossi, H. Dong, and K. Kansanen, "Time-domain oversampled OFDM communication in doubly-selective underwater acoustic channels," IEEE Commun. Lett., vol. 19, no. 6, pp. 1081-1084, Jun. 2015.

[13] S. Beygi and U. Mitra, "Multi-scale multi-lag channel estimation using low rank approximation for OFDM," IEEE Trans. Signal Process., vol. 63, no. 18, pp. 4744-4755, Sept. 2015.

[14] S. F. Mason, C. R. Berger, S. Zhou, and P. Willett, "Detection, synchronization, and doppler scale estimation with multicarrier waveforms in underwater acoustic communication," IEEE J. Sel. Areas Commun., vol. 26, no. 9, pp. 1638-1649, Dec. 2008.

[15] Y. Chen, L. Zou, A. Zhao, and J. Yin, "Null subcarriers based Doppler scale estimation for multicarrier communication over underwater acoustic non-uniform Doppler shift channels," in Proc. 2016 IEEE/OES China Ocean Acoustics, pp. 1-6, Jan. 2016.

[16] H. Nouri, M. Uysal and E. Panayirci, "Information theoretical performance analysis and optimisation of cooperative underwater acoustic communication systems," in IET Communications, vol. 10, no. 7, pp. 812-823, 5 5 2016.

[17] L. Zhang, J. Han, J. Huang, and M. Brandt-Pearce, "OFDM transmission over time-varying channel with self interference cancellation," in Proc. IEEE International Conference on Signal Processing, Communications and Computing, pp. 743-746, 2014.

 ISBN: 978-1-61208-572-2